ANALYSIS ON THE SOURCE AND SINK OF KINETIC ENERGY OF ATMOSPHERIC 30—60 DAY PERIOD OSCILLATION AND THE PROBABLE CAUSES*

Li Qingquan (李清泉)

Department of Geophysics, Peking University, Beijing 100871

and *Zhu Qiangen* (朱乾根)

Nanjing Institute of Meteorology, Nanjing 210044

Received August 15, 1994; revised June 18, 1995

ABSTRACT

Based on ECMWF daily grid point data in summer (May—August), 1981, the distribution features of the source and sink of kinetic energy of atmosphere 30—60 day oscillation, including its horizontal distribution characteristics and its vertical structure characteristics, are investigated systematically with diagnostic analysis methods over a latitude belt between 80°N and 60°S. Also, the probable reasons for the existence of the source and sink of low frequency kinetic energy (LFKE) are discussed preliminarily. Results show that the horizontal distribution of the sources and sinks of kinetic energy of atmospheric 30—60 day oscillation is extremely different. The significant sources and sinks of LFKE mainly exist in the oceans and the coastal regions of continents or islands in the mid-high latitudes. It is also found that, in the vertical direction, the sources and sinks of kinetic energy of 30—60 day oscillation display barotropic structure in the mid-high latitudes of both hemispheres, but dispaly baroclinic structure in the equtorial region, and in the horizontal direction, the sources and sinks mainly display zonal wave-like distribution. The source and sink of LFKE are determinded by ageostrophic wind effect, frictional effect, interaction between sub-grid-scale systems, nonlinear interaction, and the flux-divergence of LFKE transported by transient wind. There are some regional reasons for the generation of sources and sinks which are not completely identical in different areas.

Key words: low frequency oscillation, atmospheric energy, source and sink of kinetic energy, 30—60 day oscillation

I. INTRODUCTION

Up to now, there have been a number of researches on atmospheric energy in low-frequency range (Li 1990; Chen 1985; Krishnamurti, et al. 1985; He 1988). By using First Global Atmospheric Research Program Global Experiment (FGGE) data in summer 1979, He et al. (1986) studied the features of energy budget over tropical regions and pointed out that the monsoon regions of Asia is the main area where the kinetic energy of 30—60 day oscillation is generated during summer. Wu and Luo (1987) computed the energetics characteristics of low-frequency oscillation over tropics for April—June, 1981. Later, Xu and Lin (1990)

* This work is supported by the National Natural Science Foundation of China.

studied the mean values of the elements u, v, T, z in the regions near the equator (5°S—5°N, 80°E — 120°E) and in mid-latitude (40°N — 60°N, 140°E — 180°E), and then analyzed the evolution of kinetic energy of 30 — 60 day period oscillation and its probable maintenance mechanism. However, those previous researches did not discuss the issue on the source and sink of LFKE specially. Recently, Zhu et al. (1994) have studied some features of the source and sink of LFKE primarily. But their work is merely limited in mid-high latitude regions during boreal winter and does not touch upon the cause of the generation of source and sink.

In this paper, by studying source and sink of the kinetic energy of atmospheric low-frequency oscillation over a latitude belt between 80°N and 60°S, the distribution features of the source and sink are revealed. And by analyzing various terms in the equations of the source and sink of LFKE, the probable causes for the existences of the source and sink are studied primarily.

II. DATA AND COMPUTATIONAL METHODS

The data used in this paper were extracted from the ECMWF' s objectively analyzed dataset from May 1 to August 31 (123 days in all), 1981. The chosen meteorological elements are meridional and zonal wind (u, v), geopotential height (z), temperature (T) and vertical velocity (ω) on seven layers (i. e., 100, 850, 700, 500, 300, 200 and 100 hPa). The covered area is a latitude belt between 80°N and 60°S, with a $5° \times 5°$ grid spacing.

In order to obtain the 30 — 60 day low-frequency component, a one-step Butterwerth filter proposed by Murakami (1979) is utilized to carry out low-frequency band-pass filtering. Because the vertical component of low-frequency wind is much less than its zonal component, the LFKE can be expressed as

$$\tilde{k} = \frac{1}{2}(\tilde{u}^2 + \tilde{v}^2), \tag{1}$$

where $\tilde{u}$ and $\tilde{v}$ are the values of 30—60 day band-pass filtered u and v, respectively. We define the individual derivative of LFKE ($\mathrm{d}\tilde{k}/\mathrm{d}t$) as its apparent source (or sink), called source (or sink) for short. When the individual derivative of LFKE of an air parcel is positive ($\mathrm{d}\tilde{k}/\mathrm{d}t > 0$), the air parcel is a sink of low-frequency energy, while when the individual derivative is negative ($\mathrm{d}\tilde{k}/\mathrm{d}t < 0$), the air parcel is a sink of LFKE. According to continuity equation, $\mathrm{d}\tilde{k}/\mathrm{d}t$ can be written as

$$\frac{\mathrm{d}\tilde{k}}{\mathrm{d}t} = \frac{\partial \tilde{k}}{\partial t} + \nabla \cdot \boldsymbol{V}\tilde{k}. \tag{2}$$

Take the seasonal, which is 123 days in this paper, mean of Eq. (2), we get

$$\langle\frac{\mathrm{d}\tilde{k}}{\mathrm{d}t}\rangle = \langle\frac{\partial \tilde{k}}{\partial t}\rangle + \langle\nabla \cdot \boldsymbol{V}\tilde{k}\rangle, \tag{3}$$

where "$\langle\ \rangle$" denotes seasonal mean. Considering that $\langle\partial \tilde{k}/\partial t\rangle$ can be ignored compared with the flux divergence of LFKE (the computed results show that $\langle \partial \tilde{k}/ \partial t\rangle$ is about 3 orders of magnitude less than $\langle\nabla \cdot \boldsymbol{V}\tilde{k}\rangle$). As far as seasonal mean, we can use $\langle\nabla \cdot \boldsymbol{V}\tilde{k}\rangle$ to take the place of $\langle\nabla \cdot \boldsymbol{V}\tilde{k}\rangle$ approximately, that is,

$$\langle\frac{\mathrm{d}\tilde{k}}{\mathrm{d}t}\rangle \approx \langle\nabla \cdot \boldsymbol{V}\tilde{k}\rangle. \tag{4}$$

Correspondingly, the source and the sink of LFKE are defined as the following, respectively. When 3-D flux divergence of LFKE is divergent, it is called a source of LFKE. On the contrary, when 3-D flux divergency LFKE is convergent, with LFKE being transported in, it is called a sink of LFKE.

Given $\boldsymbol{V}^*$ is the deviation of seasonal mean wind, transient wind, we can obtain

$$\nabla \cdot \boldsymbol{V} \tilde{k} = \nabla \cdot (\langle \boldsymbol{V} \rangle + \boldsymbol{V}^*)\tilde{k} = \nabla \cdot \langle \boldsymbol{V} \rangle \tilde{k} + \nabla \cdot \boldsymbol{V}^* \tilde{k},$$

$$\text{or} \quad \nabla \cdot \boldsymbol{V} \tilde{k} = \nabla \cdot \langle \boldsymbol{V} \rangle \tilde{k} + \nabla \cdot \boldsymbol{V}^* \tilde{k}. \tag{5}$$

According to the work of He et al. (1986), the kinetic energy equation which controls 30—60 day oscillations is

$$\frac{\partial \tilde{k}}{\partial t} = - \nabla \cdot \langle \boldsymbol{V} \rangle \tilde{k} + I(\langle k \rangle, \tilde{k}) + I(k^*, \tilde{k}) + F(\tilde{\Phi}) + I(p,\tilde{k}) + R(\tilde{k}). \tag{6}$$

Utilizing Eqs. (2), (5) and (6), we obtain

$$\frac{\mathrm{d}\tilde{k}}{\mathrm{d}t} = I(\langle k \rangle, \tilde{k}) + I(k^*, \tilde{k}) + F(\tilde{\Phi}) + I(p,\tilde{k}) + \nabla \cdot \boldsymbol{V}^* \tilde{k} + R(\tilde{k}). \tag{7}$$

After taking seasonal mean of Eq. (7) and using Eq. (4), we get

$$\begin{aligned}\langle \nabla \cdot \boldsymbol{V}\tilde{k} \rangle = & \langle I(\langle k \rangle, \tilde{k}) \rangle + \langle I(k^*, \tilde{k}) \rangle + \langle F(\tilde{\Phi}) \rangle + \langle I(p,\tilde{k}) \rangle \\ & + \langle \nabla \cdot \boldsymbol{V}^* \tilde{k} \rangle + \langle R(\tilde{k}) \rangle. \end{aligned} \tag{8}$$

Formula (8) is the very basic equation that we use to compute and investigate the source and sink of low-frequency kinetic energy in this paper. Here,

$$\langle \nabla \cdot \boldsymbol{V}\tilde{k} \rangle = \overline{\frac{\partial u\tilde{k}}{\partial x} + \frac{\partial v\tilde{k}\cos\varphi}{\cos\varphi\,\partial y} + \frac{\partial \omega\tilde{k}}{\partial p}},$$

$$\begin{aligned}\langle I(\langle k \rangle, \tilde{k}) \rangle = & - \overline{\left[\tilde{u}\tilde{u} \frac{\partial \langle u \rangle}{\partial x} + \tilde{u}\tilde{v} \frac{\partial \langle u \rangle}{\partial y} + \tilde{u}\tilde{\omega} \frac{\partial \langle u \rangle}{\partial p} - \left(\frac{\tan\varphi}{a} \right) \cdot \tilde{u}\tilde{u} \langle v \rangle \right]} \\ & - \overline{\left[\tilde{u}\tilde{v} \frac{\partial \langle v \rangle}{\partial x} + \tilde{v}\tilde{v} \frac{\partial \langle v \rangle}{\partial y} + \tilde{v}\tilde{\omega} \frac{\partial \langle v \rangle}{\partial p} + \left(\frac{\tan\varphi}{a} \right) \cdot \tilde{u}\tilde{v} \langle u \rangle \right]},\end{aligned}$$

$$\begin{aligned}\langle I(k^*, \tilde{k}) \rangle = & - \overline{\left[\tilde{u}\left(\frac{\partial \widetilde{u^* u^*}}{\partial x} + \frac{\partial \widetilde{u^* v^*} \cos^2\varphi}{\cos^2\varphi\,\partial y} + \frac{\partial \widetilde{u^* \omega^*}}{\partial p} \right) \right.} \\ & \overline{\left. + \tilde{v}\left(\frac{\partial \widetilde{u^* v^*}}{\partial x} + \frac{\partial \widetilde{v^* v^*} \cos\varphi}{\cos\varphi\,\partial y} + \frac{\partial \widetilde{v^* \omega^*}}{\partial p} + \frac{\tan\varphi}{a} \cdot \widetilde{u^* u^*} \right) \right]},\end{aligned}$$

$$\langle F(\tilde{\Phi}) \rangle = - \overline{\left(\frac{\partial \tilde{u}\tilde{\Phi}}{\partial x} + \frac{\partial \tilde{v}\tilde{\Phi}\cos\varphi}{\cos\varphi\,\partial y} + \frac{\partial \tilde{\omega}\tilde{\Phi}}{\partial p} \right)},$$

$$\langle I(p,\tilde{k}) \rangle = - \overline{\frac{R}{p} \cdot \tilde{\omega}\tilde{T}},$$

$$\langle \nabla \cdot \boldsymbol{V}^* \tilde{k} \rangle = \overline{\frac{\partial u^* \tilde{k}}{\partial x} + \frac{\partial v^* \tilde{k} \cos\varphi}{\cos\varphi\,\partial y} + \frac{\partial \omega^* \tilde{k}}{\partial p}},$$

and

$$\langle W(\tilde{\Phi}) \rangle = - \overline{\left[\tilde{u} \frac{\partial \tilde{\Phi}}{\partial x} + \tilde{v} \frac{\partial \tilde{\Phi}}{\partial y} \right]} = \langle F(\tilde{\Phi}) \rangle + \langle I(p,\tilde{k}) \rangle, \tag{9}$$

$$\langle I(\tilde{k}) \rangle = \langle I(k^*, \tilde{k}) \rangle + \langle I(\langle k \rangle, \tilde{k}) \rangle, \tag{10}$$

so

$$\langle \nabla \cdot \boldsymbol{V}\tilde{k} \rangle = \langle W(\tilde{\Phi}) \rangle + \langle I(\tilde{k}) \rangle + \langle \nabla \cdot \boldsymbol{V}^* \tilde{k} \rangle + \langle R(\tilde{k}) \rangle. \tag{11}$$

In the above formulas, the horizontal line "——" denotes the 4-month (May—August) mean value, also called seasonal mean value; the wave curve "$\sim$" denotes 30—60 day's filtered data, and the asterisk "$*$" denotes the deviation to the seasonal mean value. $W(\tilde{\Phi})$ is the ageostrophic wind forcing, namely the work done by pressure-gradient force; $F(\tilde{\Phi})$ is horizontal or vertical divergence of potential energy; $I(p,\tilde{k})$ is conversion between potential energy and kinetic energy; $I(\tilde{k})$ is nonlinear term; $I(\langle k\rangle,\tilde{k})$ is nonlinear interaction between zonal mean wind field and low-frequency wind field; $I(k^*,\tilde{k})$ is nonlinear interaction between 30—60 day perturbations and transient disturbances, which is the rate at which momentum is transferred to 30—60 day perturbation through nonlinear coupling among various kinds of periodic perturbations. $\nabla \cdot \boldsymbol{V}^* \tilde{k}$ is the flux divergence of LFKE by transferred transient winds. $R(\tilde{k})$ is residual term, which comprises general viscous frictional dissipation and kinetic energy exchange between sub-grid scales. In the balance equation of source and sink, $R(\tilde{k})$ is computed as remainder, so it contains observational and computational error inevitably.

Furthermore, all the terms stated above are integrated in the whole troposphere, namely,

$$\int_{z_s}^{z_t} \rho A \mathrm{d}z = \frac{1}{g}\int_{p_t}^{p_s} A \mathrm{d}p.$$

For convenience, we take $p_s = 1000$ hPa, $p_t = 100$ hPa, where A indicates the flux divergence of atmospheric LFKE or any of the other physical variables.

III. THE DISTRIBUTION FEATURES OF SOURCE AND SINK OF KINETIC ENERGY OF 30—60 DAY PERIOD OSCILLATION

Figure 1 depicts the horizontal distribution of mean source and sink of LFKE integrated in the whole troposphere in summer 1981. It is noted: (1) The centers of strong sources or sinks mainly lie over the mid-high latitude regions north of 30°N and south of 20°S, which appear wave-like distribution with the central value of source or sink smaller in the low-latitude region. The situation is similar to the distribution of LFKE (figure omitted). The variance ratio of LFKE to total kinetic energy in low-latitudes is big relative to that in high-latitudes. Therefore, although its value in the low-latitude region is small, the contribution of the source and sink of LFKE is significant. (2) The centers of sources are accompanied by those of higher LFKE (the black dots in Fig. 1). It may mean that after LFKE is generated in its

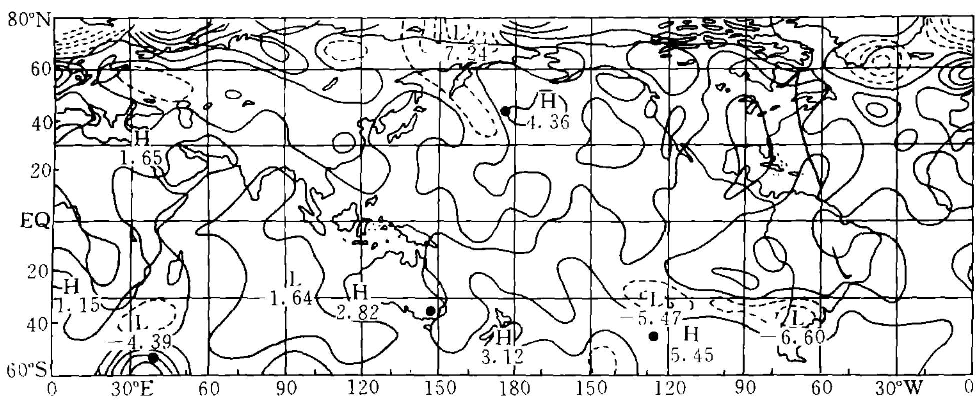

Fig. 1. The horizontal distribution of mean source and sink integrated in the whole troposphere (solid line indicates source, and dashed line indicates sink). The contour interval is 2.0×10^{-1} W m^{-2}.

source, it accumulates there at first, and then is transported to the sink of LFKE. (3) In the mid-latitudes of the Northern Hemisphere, sources mainly exist over oceans (North Pacific and North Atlantic Oceans), and sinks mainly exist over continents (Eurasian Continent and North America Continent). Conversely, in the mid-latitudes of the Southern Hemisphere, sources mainly exist over continents (South Africa, Australia and South America), and sinks mainly exist over oceans (Indian Ocean, South Pacific and South Atlantic Oceans). (4) The monsoon area of Asia and Australia is mainly dominated by sources of LFKE, and the monsoon area of Africa is mainly dominated by sinks. Generally speaking, in mid-high latitude area, the centers of source and sink mainly lie over the oceans and the coastal regions of continents or islands, while the sources and sinks in inland areas are relatively weak. It may imply that the interaction between ocean and atmosphere plays an important role to the source and sink of atmospheric LFKE as well as low-frequency oscillation.

The distribution curves of LFKE source and sink averaged in different heights and different latitudes (shown in Fig. 2) display clearly that the source and sink mainly appears 3 to 4 waves in zonal direction in the high-latitudes of the Northern Hemisphere (60°N—70°N, see Fig. 2a), 5 to 6 waves in mid-latitudes of both Hemispheres (40°S (N)—50°N (S), see Figs. 2b and 2d), and 6 to 7 waves near the equator (5°N—5°S, see Fig. 2c). The maximum amplitude of wave motion increases with increasing latitude. In the same latitude, source and sink in the Southern Hemisphere (during winter-time) are stronger than those in the Northern Hemisphere (during summer-time). It is also shown that the distribution of source and sink has a great differences in different latitudes. Apart from individual areas, the source and sink of LFKE are nearly identical from upper to lower level in the vertical direction, reflecting the feature of barotropic disturbance, while it appears baroclinic structure near the equator except the region between 100°W and 120°W.

IV. ANALYSIS OF THE REASON FOR EXISTENCE OF LOW-FREQUENCY ENERGY SOURCE AND SINK

From Eq. (11), it can be seen that the mean sink and source ($\langle \nabla \cdot \boldsymbol{V}\tilde{k}\rangle$) are determined by the four terms on the right side of the equation. They are ageostrophic wind term $\langle W(\tilde{\Phi})\rangle$, nonlinear term $\langle I(\tilde{k})\rangle$, residual term $\langle R(\tilde{\Phi})\rangle$ and the flux divergence of LFKE transported by transient wind. Figure 3 presents the horizontal distribution of each term integrated in the whole troposphere during summer 1981.

Figure 3a depicts the horizontal distribution of nonlinear effect $\langle I(\tilde{k})\rangle$. It is obvious that the centers with larger value of $\langle I(\tilde{k})\rangle$ lie in the mid-latitudes of the Southern Hemisphere and the high-latitudes of the Northern Hemisphere, while the value of $\langle I(\tilde{k})\rangle$ is smaller in the low-latitudes of the Northern Hemisphere and near the equator. The nonlinear effect in the low-middle latitude regions of the Southern Hemisphere is larger than that in the Northern Hemisphere. A comparison of Fig. 3 with Fig. 1 reveals that the distributions of $\langle \nabla \cdot \boldsymbol{V}^{*}\tilde{k}\rangle$ and of $\langle I(\tilde{k})\rangle$ are roughly "out-of-phase", that is to say, the source (sink) of LFKE corresponds to negative (positive) $\langle I(\tilde{k})\rangle$. It illustrates that nonlinear effect plays a negative role in generating source and sink of LFKE. Certainly, there are some exceptions. For example, in the high-latitude region of North America, Alaska and Bering, nonlinear effect is in favor of the existence of source and sink of LFKE.

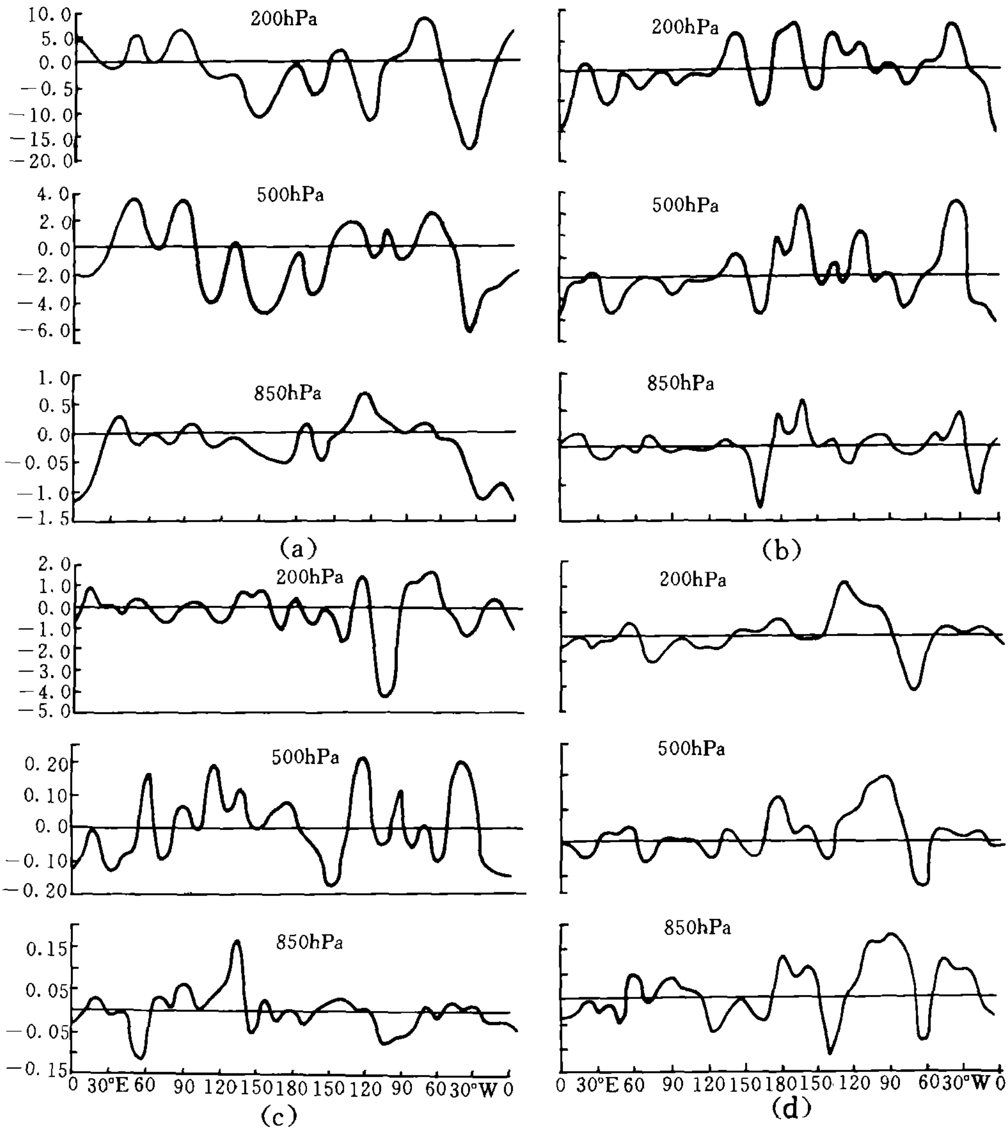

Fig. 2. The zonal distribution curves of mean source and sink (unit is $10^{-5}m^2 s^{-3}$). (a) 60°N—70°N; (b) 40°N—50°N; (c) 5°N—5°S; (d) 40°S—50°S.

Figure 3b shows the flux divergence of LFKE transferred by transient wind ($\boldsymbol{V}^*$). Comparing Fig. 3b with Fig. 1, we find that contrary to $\langle I(\tilde{k})\rangle$, the distributions of $\langle \nabla \cdot \boldsymbol{V}^* \tilde{k}\rangle$ and of $\langle \nabla \cdot \boldsymbol{V}\tilde{k}\rangle$ are roughly "in phase", that is to say, the source (sink) of LFKE corresponds to positive (negative) $\langle \nabla \cdot \boldsymbol{V}^* \tilde{k}\rangle$. Apart from the West and South Asia, the high-latitude region of North America, East Australia and part of South Pacific Ocean, where sources (sinks) are corresponding to the regions with negative (positive) value of $\langle \nabla \cdot \boldsymbol{V}^* \tilde{k}\rangle$, in most of other regions, LFKE is transferred out (in) its source (sink) by transient winds, so it favours the existence of source and sink. In addition, as shown in Fig. 3b, the value of $\langle \nabla \cdot \boldsymbol{V}^* \tilde{k}\rangle$ is smaller in the low-latitudes of the Northern Hemisphere and near the equator, but is larger in other regions.

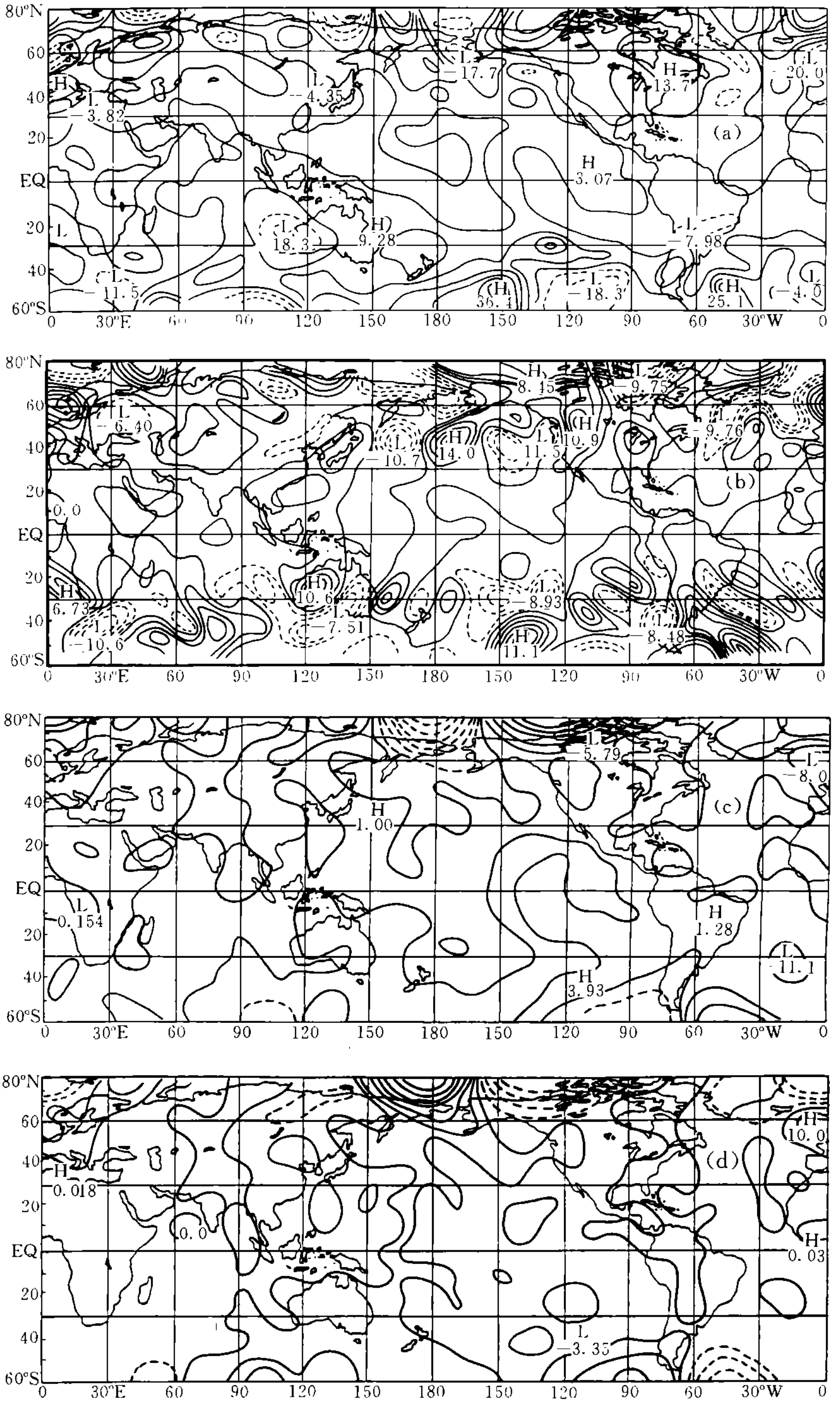

Fig. 3. The computed results of the four terms on the right side of Eq. (11). Solid lines indicate positive values, and dashed lines indicate negative values. (a) $\langle I(\tilde{k})\rangle$, at contour interval 0.6×10^{-1} W m^{-2}; (b) $\langle \nabla\cdot \boldsymbol{V}^{*}\tilde{k}\rangle$, at contour interval 0.2×10^{-1} W m^{-2}; (c) $\langle W(\tilde{\Phi})\rangle$, at contour interval 6.0 W m^{-2}; (d) $\langle R(\tilde{k})\rangle$, at contour interval 6.0 W m^{-2}.

Figure 3c shows the distribution of ageostrophic wind effect $\langle W(\tilde{\Phi})\rangle$. Obviously, the ageostrophic wind effect in high-latitudes is one order of magnitude larger than that in mid-latitudes, while it is one order of magnitude larger in mid-latitudes than in low-latitudes. The minimum (negative) and the maximum (positive) of $\langle W(\tilde{\Phi})\rangle$ appear over East Siberia-Bering and the northwest part of North America and the Arctic Ocean nearby, respectively. From Formula (11), one knows that when ageostrophic wind forcing (also called the term of the work done by pressure gradient force) is positive, it is favorable to the generation of source, but when it is negative, it is favorable to the generation of sink. A comparison of Fig. 3c with Fig. 1 indicates that the positive (negative) value of $\langle W(\tilde{\Phi})\rangle$ is corresponding to the source (sink) in most areas, that is to say, that positive (negative) work done by pressure gradient force is advantageous to the existence of the source (sink) of LFKE in those regions. However, in other areas, such as North Europe and coastal region and the high-latitude region of Asia, the negative (positive) $\langle W(\tilde{\Phi})\rangle$ value is corresponding to the source (sink) of LFKE, namely the pressure gradient force term plays a negative role in generating source and sink.

Figure 3d shows the distribution of residual term $\langle R(\tilde{k})\rangle$. As mentioned earlier, the residual term comprises frictional effect, interaction between sub-grid-scale systems and computational errors. Generally speaking, the computational error is smaller, while the frictional effect and the interaction between sub-grid-scale systems play major roles in the term $\langle R(\tilde{k})\rangle$. Frictional effect dissipates kinetic energy and plays a negative (positive) role in generating source (sink), so its value is usually negative. But the value of the interaction between sub-grid-scale systems may be positive or negative. Therefore, the sign of the term $\langle R(\tilde{k})\rangle$ can, in some extent, represent the relative strength. When the value of $\langle R(\tilde{k})\rangle$ is negative, it is probable that both of the two terms are negative, and the interaction between sub-grid-scale systems is positive, but it is weaker than the frictional effect. When the value of $\langle R(\tilde{k})\rangle$ is positive, because frictional effect is negative, the interaction between sub-grid-scale systems must be positive and its value must be larger than the absolute value of the frictional forcing. Therefore, the term $\langle R(\tilde{k})\rangle$ plays a net positive (negative) role in generating source (sink) of LFKE.

Figure 3d exhibits that $\langle R(\tilde{k})\rangle$ in high-latitudes is one order of magnitude larger than in mid-latitudes, while that in mid-latitudes is one order of magnitude larger than in low-latitudes. The positive maximum and the negative maximum of $\langle R(\tilde{k})\rangle$ exist over East Siberia-Bering and the western part of North America and its coastal regions (the North Pacific and the Arctic Oceans and the surrounding), respectively. Most areas of the global latitude belt are the regions with the negative value of $\langle R(\tilde{k})\rangle$, which play a negative (positive) role to the existence of source (sink). However, in some areas, such as Northwest Europe, West Asia (including Bay of Bengal), East Siberia-Bering and the most regions of the North Pacific Ocean in mid-latitudes, the value of $\langle R(\tilde{k})\rangle$ is positive. Therefore, the interaction between sub-grid-scale systems is of a larger positive value and the term $\langle R(\tilde{k})\rangle$ plays a positive (negative) role in generating sources (sinks).

Comparing Fig. 3c with Fig. 3d, we find that $\langle R(\tilde{k})\rangle$ and $\langle W(\tilde{\Phi})\rangle$ are of the same order of magnitude. They are one order of magnitude larger than $\langle \nabla \cdot V\tilde{k}\rangle$ and $\langle I(\tilde{k})\rangle$ in high-latitude regions, and the distributions of $\langle W(\tilde{\Phi})\rangle$ and of $\langle R(\tilde{k})\rangle$ are nearly unanimously "out-of-phase", especially in the mid-high latitudes of the Northern Hemisphere. Therefore, we suppose that $\langle W(\tilde{\Phi})\rangle$ and $\langle R(\tilde{k})\rangle$ compensate and counteract mutually. When $\langle W(\tilde{\Phi})\rangle$ is positive, with pressure-force doing positive work and $\langle W(\tilde{\Phi})\rangle$ favoring the existence of source, $\langle R(\tilde{k})\rangle$ is negative, and the residual term (including frictional effect and interaction between sub-grid-scale systems) dissipates kinetic energy, which partly or totally offsets the positive effect of $\langle W(\tilde{\Phi})\rangle$ and makes this region be a source or a sink of LFKE. When $\langle W(\tilde{\Phi})\rangle$ is negative, with pressure-force dissipating kinetic energy and $\langle W(\tilde{\Phi})\rangle$ not favoring the existence of sink, $\langle R(\tilde{k})\rangle$ is positive, and the interaction between sub-grid-scale systems is stronger than the frictional dissipation effect. The stronger interaction between sub-grid-scale systems partly or totally compensates the kinetic energy that is dissipated through pressure-force doing regative work, which makes the region be a sink or a source of LFKE.

Let us turn our attention to a more detail discussion in which the ageostrophic wind term $\langle W(\tilde{\Phi})\rangle$ is divided into the term of the convergence or divergence of potential energy $\langle F(\tilde{\Phi})\rangle$ and the term of the conversion of potential energy ($\langle I(p,\tilde{k})\rangle$) (as shown in Formula (9)), and the nonlinear term $\langle I(\tilde{k})\rangle$ is divided into the nonlinear interaction between transient disturbance and 30—60 day oscillation ($\langle I(k^*,\tilde{k})\rangle$) and the barotropic nonlinear interaction between basic flow and 30—60 day oscillation $\langle I(\langle k\rangle,\tilde{k})\rangle$ (as shown in Formula (10)).

Figure 4 presents the distribution of $\langle F(\tilde{\Phi})\rangle$ and $\langle I(p,\tilde{k})\rangle$ integrated in the whole troposphere. By comparing Figs. 4a, 4b with Fig. 3c, we find that $\langle F(\tilde{\Phi})\rangle$ and $\langle W(\tilde{\Phi})\rangle$ are of the same order of magnitude, and their distributions are almost completely identical, excepting that there are some changes in the value of the centers. In the mid-high latitude

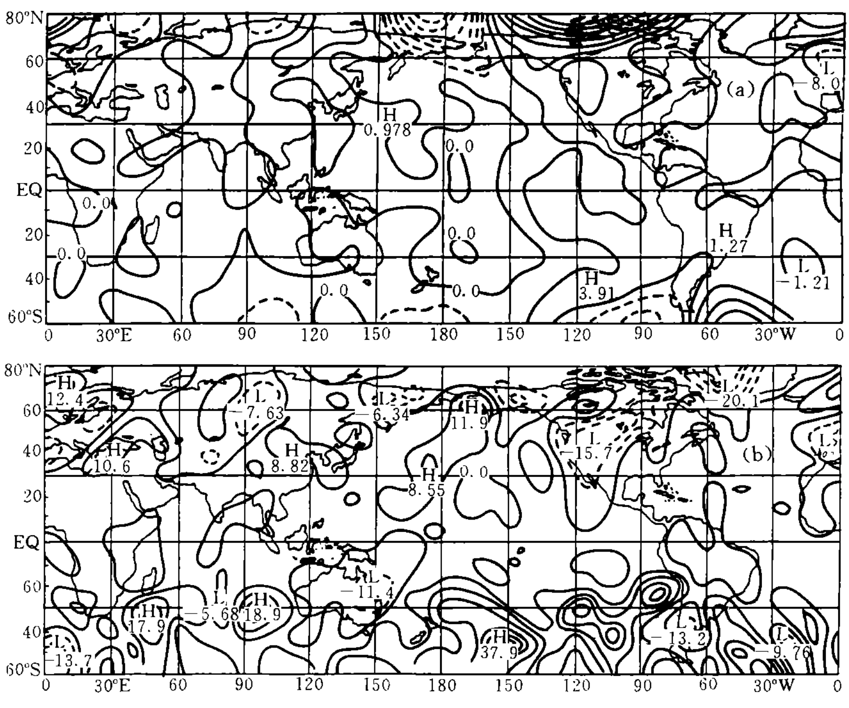

Fig. 4. The computed result: (a) $\langle F(\tilde{\Phi})\rangle$ (the contour interval is 5.0 W m^{-2}) and (b) $\langle I(p,\tilde{\Phi})\rangle$ (the contour interval is 4×10^{-2} W m^{-2}).

area, the value of $\langle W(\tilde{\Phi})\rangle$ and $\langle F(\tilde{\Phi})\rangle$ is obviously 1 to 2 orders of magnitude larger than that of $\langle I(p, \tilde{k})\rangle$. It suggests that during pressure force doing work, the term of the convergence or divergence of potential energy plays an important role, that is to say, when potential energy is convergent, pressure force does positive work, while when it is divergent, pressure force does negative work.

In Fig. 4b, $\langle I(p, \tilde{\Phi})\rangle$ is greater in the mid-high latitudes of the Northern Hemisphere (30°N—80°N) and in the low-middle latitudes of the Southern Hemisphere (20°S—60°S), but it is smaller in the equator and the low-latitude regions (30°N — 20°S). A comparison of Fig. 4b with Fig. 1 reveals that the centers with positive value of $\langle I(p,\tilde{\Phi})\rangle$ mainly lie nearby the three oceans, Bering, Red Sea-Mediterranean Sea and Mongolia. In those regions, there is remarkable conversion from effective potential energy to LFKE, which is advantageous (disadvantageous) to the existence of LFKE' s source (sink). The centers with the negative value of $\langle I(p,\tilde{k})\rangle$ mainly lie over the continents of both Hemispheres, where LFKE is significantly dissipated, which is advantageous (disadvantageous) to the existence of sink (source).

Figure 5 depicts the distribution of $\langle I(k^*,\tilde{k})\rangle$ and $\langle I(\langle k\rangle,\tilde{k})\rangle$ integrated in the whole troposphere. Comparing Fig. 5 with Fig. 3a, it is easy for us to see that the distributions of $\langle I(k^*,\tilde{k})\rangle$ and $\langle I(\tilde{k})\rangle$ are very similar in mid-high latitudes. It suggests that the nonlinear interaction between transient wind and 30—60 day osicillation has an important contribution to nonlinear effect in mid-high latitudes, which is unfavorable to the existence of source and sink. However, the distribution of $\langle I(\langle k\rangle,\tilde{k})\rangle$ in mid-high latitudes of the Northern Hemisphere

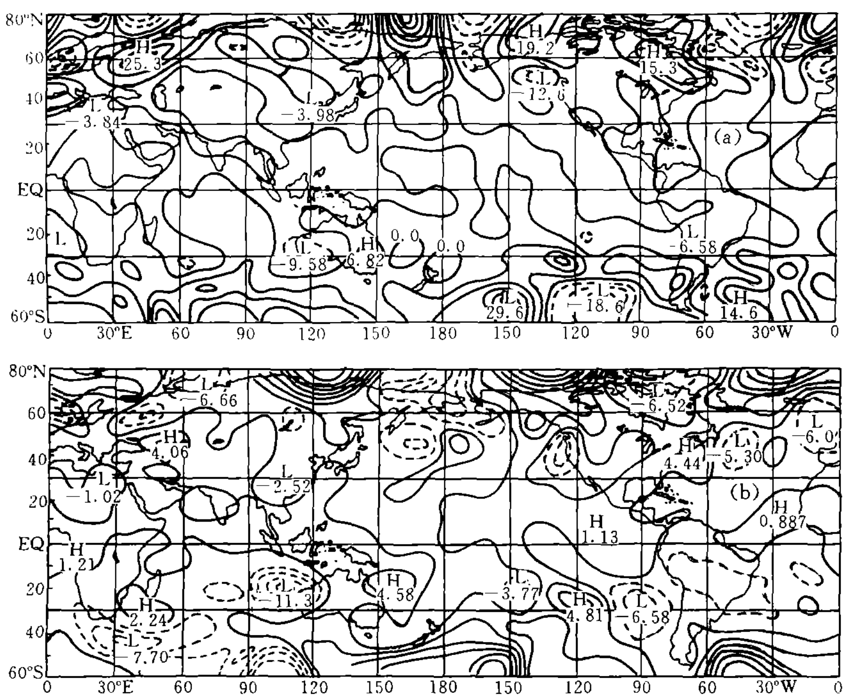

Fig. 5. The computed results: (a) $\langle I(k^*,\tilde{k})\rangle$ (the contour interval is 5.0×10^{-1} W m^{-2}) and (b) $\langle I(\langle k\rangle,\tilde{k})\rangle$ (the contour interval is 2.0×10^{-1} W m^{-2}).

exhibits a revers situation, which suggests that the nonlinear interaction between zonal mean winds and low-frequency winds is favorable to the existence of the source and sink of LFKE (but its contribution is smaller).

V. CONCLUSION

Based on the above analyses, we can draw conclusions as follows:

(1) As far as in the global range, the horizontal distribution of source and sink of kinetic energy of atmospheric 30—60 day oscillation is extremely different. Generally speaking, the regions with pronounced soures and sinks (or their centers) mainly lie over the oceans and the coastal regions of continents or islands in the mid-high latitudes, while the sources and sinks of LFKE in inland areas are relatively weak. It may imply that the interaction between ocean and atmosphere plays an important role in the source and sink of LFKE as well as low-frequency oscillation.

(2) Except in individual regions, in the vertical direction, the source and sink of kinetic energy of atmospheric 30 — 60 day oscillation display barotropic structure in the mid-high latitudes of both Hemispheres, but display baroclinic structure in the equatorial region. Moreover, the source and sink of LFKE mainly display zonal wave-like distribution in the horizontal direction, and the wave number decreases with increasing latitude. The maximum amplitude of wave motion increases with increasing height and latitude.

(3) The source and sink of LFKE are mainly determined by the frictional effect and the interaction between sub-grid-scale systems of the residual term and the ageostrophic wind effect, which on one hand, maintain the source and sink of LFKE, on the other hand, counteract each other and compensate each other. In most regions of global range, ageostrophic wind term plays a positive role in the generation of source and sink of LFKE, and residiual term plays a negative (positive) role in generating the source (sink) of LFKE. Nonlinear term and the flux divergence of LFKE transported by transient wind play negative and positive roles to the generation of source and sink of LFKE, respectively. In addition, in the course of winds' doing work, the convergence or divergence of potential energy plays an important role, but in the nonlinear term, the interaction between transient wind field and 30—60 day period oscillation has made important contributions in the mid-high latitudes.

REFERENCES

Chen, T. C. (1985). On the time variation in the tropical energetics of large-scale motions during the FGGE summer, *Tellus*, **37**A: 258—276.

He Jinhai, et al. (1986). The energy budget in 40 — 50 day oscillation, *The Collection of Science and Technology of Meteorology*, China Meteor. Press, pp. 185—195 (in Chinese).

He Jinhai (1988). The transfer of physical quantities in a QDPO and its variations to the interaction between the NH and SH circulations, *Adv. Atmos. Sci.*, **5**: 107—116.

Krishnamurti, T. N. et al. (1985). Divergent, circulations on the 30—50 day time scale. *J. Atmos. Sci.*, **42**: 364—375.

Li Chongyin (1990). Some features of 30—60 day oscillation in the atmospheric circulation of the Northern Hemisphere, *Scientia Sinica*, series B, No. **7**, 764—774.

Murakamo, T. (1979). Large-scale aspects of deep convective activity over the GATA data, *Mon. Wea. Rev.*, **107**: 994—1013.

Wu Peili and Luo Huibang (1987). The preliminarily analysis on energetics of low-frequency oscillation procession in tropical troposphere. *Journal of Tropical Meteor.*, **3**: 104—111 (in Chinese).

Xu Jianjun and Lin Chunyu (1990). Diagnostic research for evolution of kinetic energy of 30—50 day period oscillation and its probable maintenance mechanism. *Journal of Tropical Meteor.*, **6**: 324—331 (in Chinese).

Zhu Qiangen et al. (1994). Some features of source and sink of kinetic energy of 30—60 day oscillation in the mid-high latitudes of the Northern Hemisphere in winter. *J. Nanjing Institute of Meteor.*, **17**: 227—284 (in Chinese).